Directivity patterns of disc transducers operating in water

Joe Wong* and Faranak Mahmoudian
wongjoe@ucalgary.ca

Introduction: In seismic physical modeling, disc-shaped piezoelectric transducers are commonly used as generators and detectors of acoustic waves in water. Even the smallest transducers have diameters which are significant fractions of a wavelength. Because of this, the radiation and reception patterns of such transducers have pronounced directivities due to wave interference effects. Physically-modeled reflection amplitudes must be corrected for the directivities before doing any AVO/AVAZ analysis.

Disc transducer are polarized electrically in the thickness direction. When used in physical modeling, the thickness direction is the vertical direction. Therefore, they radiate and respond to vertical motion. We can calculate directivity for total or vertical displacement either numerically or analytically.

Geometry: Figure 1a shows the geometry for calculating directivity. The blue semi-circle indicates receiver positions with constant distant R from the disc transducer, with R much greater than both the disc diameter D and the wavelength λ. The face of the transducer is divided up into many small areal elements each radiating with a source function of the form $\cos(kR)/R$, where $k = 2\pi/\lambda$ is the wavenumber. The receiver and source coordinates are :

$$x_r = R\sin(\theta),\ \ y_r = 0,\ z_r = R\cos(\theta),\ \ x_s = \rho\cos\phi,\ y_s = \rho\sin\phi,\ z_s = 0\ ,$$

$$|r_r - r_s| = \sqrt{(x_r - x_s)^2 + (y_r - y_s)^2 + (z_r - z_s)^2}\ .$$

Numerical method: The face of the transducer is divided up into many square areal elements (Figure 1b). Summing over all elements gives the displacement field:

$$V_r(\theta) = \sum_s \cos\left(k|r_r - r_s|\right)/|r_r - r_s|(\Delta x_s \Delta y_s)\ . \qquad (1)$$

Normalizing $V_r(\theta)$ by its maximum value gives the numerical directivity for total displacement.

Analytic method: In cylindrical coordinates, the face of the transducer is divided up into many small areal elements (Figure 1c). By integrating, we get the total displacement field:

$$U_r(\theta) \sim (\cos(kR)/R)\int_0^a [\int_0^{2\pi}\{\cos(k\rho\sin\theta\cos\phi)\}d\phi\ ]\rho d\rho\ .$$

The double integration yields the Bessel function $J_1(X)$. Normalization results in the radiation directivity for the total displacement:

$$U_r^N(\theta) = J_1(X)/X\ ,\ \ X = (\pi D\sin\theta)/\lambda\ . \qquad (2)$$

The directivities for both the numerical procedure (Equation 1) and the analytic expression (Equation2) are controlled by the dimensionless parameter D/λ (see Figure 2). The larger the value of D/λ , the more focused toward the vertical direction ($\theta = 0°$) are the directivities.

Applying directivity corrections to physically-modeled data:

Figure 3 displays a CMP gather of seismograms recorded over a scale model using the U of C Seismic Physical Modeling Facility. The model was an acrylic plastic slab immersed in water.

Figure 4 shows the reflection arrivals from the water-acrylic interface in wiggle-trace and colour-coded displays with fixed gains. The trace-to-trace relative amplitudes can be estimated by the peak-to-trough excursions.

On Figure 5a, the raw reflection amplitudes are plotted versus incident angle. On Figure 5b, the raw amplitudes have been corrected for spherical divergence and vertical-component combined directivity (accounts for both the radiation AND the reception patterns of disc transducers). They are then plotted in direct comparison with the theoretical spherical-wave and plane-wave Zoeppritz AVA predictions. The corrected experimental AVO response fits well with the spherical-wave AVO predictions for angles slightly beyond the critical angle.

Acknowledgement: This research was supported by NSERC and the industrial sponsors of CREWES.

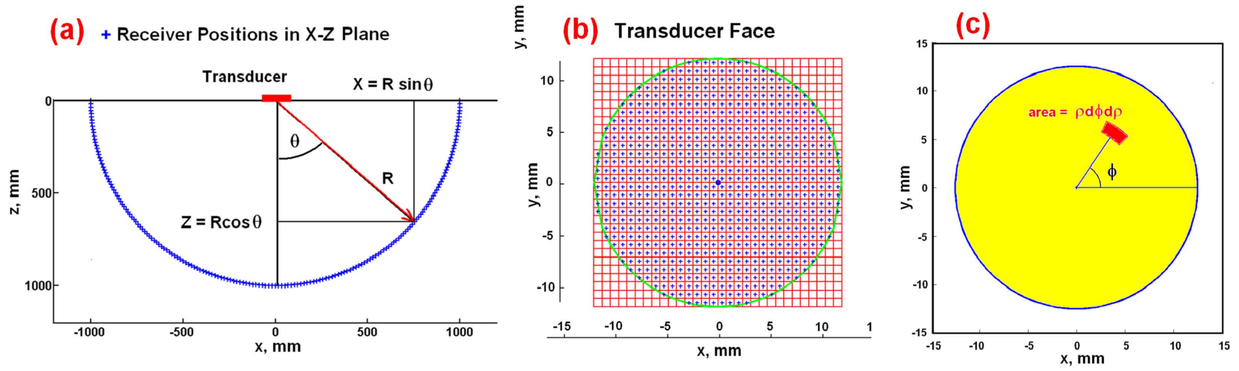

FIG. 1. (a) Geometry for calculating the radiation directivity of a disc transducer. (b) Numerical procedure: the circular face of the transducer is divided up into many small square elements, and the total displacement is the sum of Green's functions from all the elements. (c) Analytic procedure: the total displacement is obtained by integrating in cylindrical coordinates the Green's functions for all small areas on the surface of the transducer.

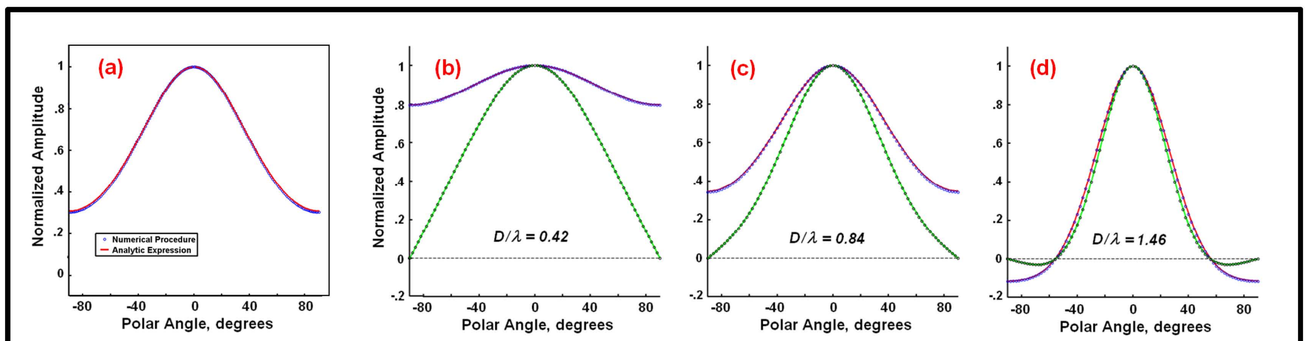

FIG 2. Directivities for total displacement from the numerical procedure (Equation 1) and the analytic expression (Equation 2) agree very closely. The lower curves on Figures 2b to 2d are the directivities for the vertical displacement, obtained by multiplying Equations 1 and 2 by cos(θ), where θ is the polar angle.

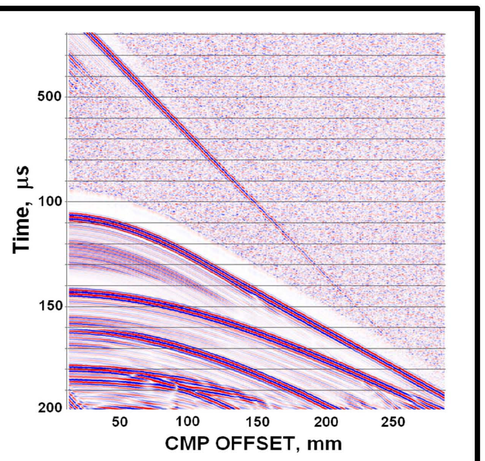

FIG 3. AGC display of a Common Midpoint Gather of modeled seismograms. The reflection starting at about 105 μs is from the water-acrylic interface

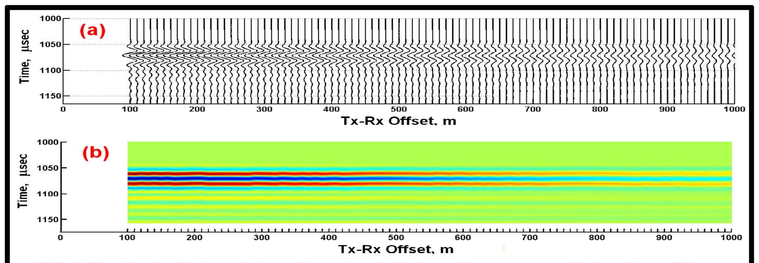

FIG 4. Fixed-gain display of the reflected arrivals from the water-acrylic interface. The arrivals have been flatted by removing the moveout of the arrival times. The reflection starting at about 105 μs is from the water-acrylic interface

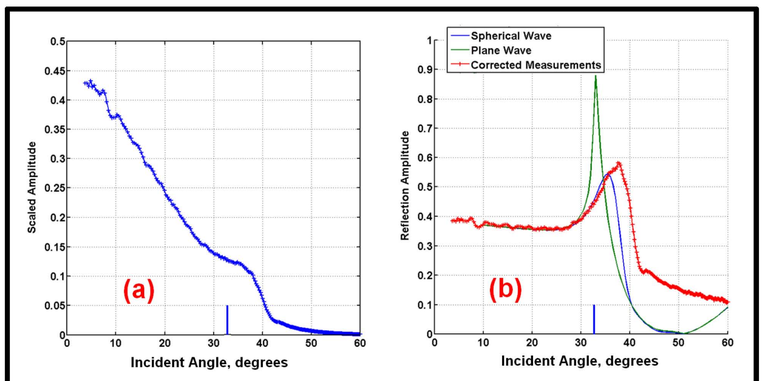

FIG. 5. (a) Raw amplitudes picked on the reflected arrivals from the water-acrylic interface. (b) Reflected amplitudes corrected for spherical divergence and combined (radiation and reception) vertical-component directivity. The short blue lines on the horizontal axes indicate the critical angle for the water-acrylic boundary.